Desalination and Water Treatment
www.deswater.com

doi: 10.5004/dwt.2018.22680

118 (2018) 342–351
June

Carbonization of corn (*Zea mays*) cob agricultural residue by one-step activation with sulfuric acid for methylene blue adsorption

Ali H. Jawad[a,*], Shaymaa Adil Mohammed[b], Mohd Sufri Mastuli[a], Mohd Fauzi Abdullah[c]

[a]*Faculty of Applied Sciences, Universiti Teknologi MARA, 40450 Shah Alam, Selangor, Malaysia, Tel. +603 55211721; emails: ahjm72@gmail.com, ali288@salam.uitm.edu.my (A.H. Jawad), Tel. +603 55436594; email: mohdsufrimastuli@yahoo.com (M.S. Mastuli)*
[b]*Department of Chemistry, College of Science, Al-Muthanna University, Iraq, Tel. +9647809400813; email: Samohammed15@gmail.com*
[c]*Faculty of Applied Sciences, Universiti Teknologi MARA, 02600 Arau, Perlis, Malaysia, Tel. +60 49882737; email: mohdfauziabd@perlis.uitm.edu.my*

Received 9 August 2017; Accepted 27 June 2018

ABSTRACT

Corn (*Zea mays*) cob, an agricultural biomass residue, was carbonized by chemical activation with H_2SO_4 and examined for its suitability as a low-cost adsorbent for methylene blue (MB) adsorption from aqueous solution. Carbonized corn cob (CCC) was characterized by a CHNS-O analysis, Fourier transform infrared spectroscopy, scanning electron microscopy, X-ray diffraction (XRD), Brunauer–Emmett–Teller, and *point-of-zero charge* (pH_{pzc}) analysis. Batch mode adsorption studies were conducted by varying operational parameters such as adsorbent dosage (0.02–0.20 g), solution pH (3–10), initial MB concentrations (50–300 mg/L), and contact time (0–360 min). The equilibrium data were well correlated by the Freundlich isotherm compared with Langmuir and Temkin models. The maximum adsorption capacity (q_{max}) of CCC for MB adsorption at equilibrium was 216.6 mg/g at 303 K. The kinetic uptake profiles were well-described by the nonlinear pseudo-first-order model. The thermodynamic adsorption parameters such as standard enthalpy ($\Delta H°$), standard entropy ($\Delta S°$), and standard free energy ($\Delta G°$) showed that the adsorption of MB onto CCC surface is endothermic in nature and spontaneous under the experimental conditions. The above-mentioned results indicate that the CCC can be feasibly employed for the removal of MB from aqueous solution.

Keywords: Carbonization; Corn cob; Low-cost adsorbent; Sulfuric acid; Adsorption; Methylene blue

1. Introduction

Wastewater from textile, rubber, paper, plastics, leather, and food industries contains dyes used to color their final products. The discharge of dye-contained wastewaters into ecosystem is a dramatic source of aesthetic pollution, eutrophication, and perturbation in aquatic life as most dyes are highly visible, stable, and unaffected by chemical, photochemical as well as biological degradation [1–3]. By definition, basic dyes are cationic species originating from positively charged nitrogen or sulfur atoms. In fact, basic dyes are named because of their affinity to basic textile materials with net negative charge [4]. Methylene blue (MB) is a basic dye with favorable water solubility and the most commonly used for dyeing of textiles and leather, printing calico, printing cotton, and biological staining methods [5]. Tinctorial value of MB is very high, even at concentration less than 1 mg/L, a noticeable coloration is detected and can be classified as toxic colorants [6]. MB has various harmful effects on human beings, such as eye irritation, gastrointestinal irritation, and nausea upon ingestion, including vomiting and diarrhea [7], so it is of utmost importance to be removed from wastewaters.

Various conventional technologies have been tested for the removal of dyes from industrial effluents and wastewaters,

* Corresponding author.

including bioremediation [8], electrochemical degradation [9], cation exchange membranes [10], Fenton chemical oxidation [11], and photocatalysis [12,13]. Most of these methods, however, pose techno-economical limitations for field-scale applications [14]. In contrast, adsorption has been proved to be a well-established and most widely used technique among other water purification processes. Adsorption-based treatment with appropriate adsorbent materials shows high performance and selectivity, flexibility and simplicity of design, convenience of operation without producing harmful by-products as well as being economically cost effective [15].

Activated carbons (ACs) are materials containing large surface area, well-developed porosity, and various functional groups. Therefore, AC has been widely utilized in versatile applications such as gas separation, solvents recovery, gas storage, super capacitors electrodes, catalyst support, adsorbent for organic and inorganic pollutants from drinking water, and so on [16]. However, the high cost of AC production limits its application in various technologies. Recognizing this economic obstacle, many investigators have made extensive efforts to identify low-cost alternatives to AC made from a range of carbonaceous precursors, such as lignocellulosic materials [17], biopolymer [18], coal [19], char [20], and fruit peels [21]. The textural properties and adsorption capacities of carbonaceous materials mainly depend on the nature of the starting material, activation method, type of activator, and preparation conditions [22].

Chemical surface modification methods are widely used to prepare hydrophilic carbonaceous materials. Hydrophilicity of the carbonaceous materials is associated essentially with the presence of oxygen containing groups on the surface such as carboxylic, phenolic, and lactonic groups. Sulfuric acid is a reagent that is frequently used to enhance oxygen content on the surface [23]. Research has demonstrated that the amount of oxygen containing surface functional groups, specific surface area, and pore structure highly depend on the concentration of activation agents. While oxygen content of carbonaceous materials usually increases with the increase of reagent concentration, the surface area and pore volume values decrease adversely [24]. Nowadays, interests are growing in the utilizing of agricultural waste and food residues as low-cost and steady sources for developing rich carbonaceous materials with multifunctional functional groups that can be potentially for removal of water pollutants.

Corn (*Zea mays*) is also known as the maize plant. The corn cobs (CCs) are the by-products generated during processing corn, which is one of the most widely planted crops in the world. It was estimated that the total yield of corn arrived 6.1×10^8 t in 2001. Only in China, the yield of corn has reached 1.2×10^8 t. Since the ratio between corn grain and CCs may reach 100:18, a large quantity of CCs were generated [25]. Modification of corn cob (CC) with sulfuric acid can produce a carbonized form of corn cob (CCC). Therefore, in this work, CC as an agricultural biomass residue material was carbonized via liquid phase oxidation with sulfuric acid to develop a low-cost and effective adsorbent for the removal of cationic dye from aqueous solution. MB was chosen as a typical cationic dye to figure out the adsorptive properties of the CCC. Sulfuric acid (H_2SO_4) is frequently used as a low-cost chemical agent for the preparation of carbonaceous adsorbents from ligno-cellulosic materials such as coconut leaves [17], mango peel [21], *Euphorbia rigida* [26], bagasse [27], almond husk [28], *Parthenium hysterophorus* [29], sunflower oil cake [30], pine-fruit shell [31], *Delonix regia* pods [32], wild carrot [33], *Ficus carica* [34], potato peel, and neem bark [35].

2. Materials and methods

2.1. Adsorbate (MB)

The cationic dye, MB was used as an adsorbate in this work. MB was purchased from R&M Chemicals, Malaysia with chemical formula $C_{16}H_{18}ClN_3S{\cdot}xH_2O$ and molecular weight 319.86 g/mol. Ultra-pure water was used to prepare all solutions.

2.2. Carbonization and characterization of CCC

CC was collected from local farmers in Penang, Malaysia. CC was first washed with water and subsequently dried at 105°C for 24 h to remove the moisture contents. The dried CC was ground and sieved to the size of 250–500 μm before mixing with concentrated H_2SO_4 (95%–98%). The mixing ratio was fixed at 1 g of dried CC powder with 1 mL of concentrated H_2SO_4 according to the method reported by Garg et al. [36]. The CCC was washed with hot distilled water until the filtrate water was clear and reached a neutral pH value. The elemental analysis was carried out using a CHNS-O analyzer (Flash 2000, Organic Elemental Analyzer, Thermo Scientific, Netherlands). The detection limits for the analyses were 0.3% for C, H, and 1.0% for S. X-ray diffraction (XRD) analysis was performed in reflection mode (Cu Kα radiation) on a PANalytical, X'Pert Pro X-ray diffractometer. Scans were recorded with a scanning rate of 0.59°/s. The diffraction angle (2θ) was varied from 10° to 90°. Textural characterization of CCC was carried out by N_2 adsorption using Micromeritics ASAP 2060, USA. Fourier transform infrared (FTIR) spectral analysis of CCC was performed on a PerkinElmer, Spectrum One in the 4,000–500 cm^{-1} wavenumber range. The surface physical morphology was examined by using scanning electron microscopy (SEM-EDX, Hitachi, TM3030Plus, Tabletop Microscope). The pH at the *point-of-zero charge* (pH_{pzc}) was estimated using a pH meter (Metrohm, Model 827 pH Lab, Switzerland), as described elsewhere [37]. pH was adjusted to a series of initial values between 2 and 12 by adding either HCl or NaOH and then CCC (0.15 g) to the solution. These were then shaken for 24 h in an isothermal water bath shaker, a revolving water bath to reach equilibrium, after which each resulting pH was measured and the initial pH (pH_o) versus the difference between the initial and final pH values (ΔpH) was plotted. The pzc was taken as the point where ΔpH = 0.

2.3. Batch adsorption experiments

The batch adsorption experiments of MB adsorption onto CCC surface were performed in a set of 250 mL Erlenmeyer flasks containing 100 mL of MB solution. The flasks were capped and agitated in an isothermal water bath shaker (Memmert, water bath, model WNB7-45, Germany) at fixed shaking speed of 110 stroke/min and 303 K until equilibrium

was achieved. Batch adsorption experiments were carried out by varying several experimental variables such as adsorbent dosage (0.02–0.2 g), pH (3–10), initial dye concentration (50–300 mg/L), and contact time (0–360 min) to determine the best uptake conditions for adsorption. The pH of MB solution was adjusted by adding either 0.10 mol/L HCl or NaOH. After mixing of the CCC-MB system, the supernatant was collected with a 0.20 μm nylon syringe filter and the concentrations of MB were monitored at a different time interval using a HACH DR 2800 Direct Reading Spectrophotometer at 661 nm, the maximum wavelength (λ_{max}) of absorption for MB. As for the thermodynamic studies, the same procedures were repeated and applied at 313, 323, and 333 K with the other parameters kept constant. The blank test was carried out in order to account for color leached by the adsorbent and adsorbed by the glass containers, blank runs with only the adsorbent in 100 mL of double distilled water and 100 mL of dye solution without any adsorbent were conducted simultaneously at similar conditions. The adsorption capacity at equilibrium, q_e (mg/g) and the percent of color removal, CR (%) of MB were calculated using Eqs. (1) and (2).

$$q_e = \frac{(C_o - C_e)V}{W} \tag{1}$$

$$\mathrm{CR}\% = \frac{(C_o - C_e)}{C_o} \times 100 \tag{2}$$

where C_o and C_e (mg/L) are the initial and equilibrium concentrations of MB, respectively, V (L) is the volume of the solution, and W (g) is the mass of dry adsorbent used. All kinetics and isotherm models were tested by performing the fitting of the experimental data to the nonlinear equations using a scientific data analysis and graphing software package, SigmaPlot 11. The best fitted model was also evaluated by nonlinear coefficient of determination (R^2) by the following equation:

$$R^2 = 1 - \frac{\sum_{n=1}^{n}\left(q_{t\cdot meas} - q_{t\cdot cal}\right)^2}{\sum_{N=1}^{N}\left(q_{t\cdot cal} - \overline{q_{t\cdot cal}}\right)^2} \tag{3}$$

3. Results and discussion

3.1. Characterization of CCC

3.1.1. Physical properties

The results of physical characterization of CCC are recorded in Table 1. The ultimate analysis indicates that CCC has a relatively high carbon and oxygen content with low surface area. The low surface area of CCC can be attributed to the high concentration of activation agent H_2SO_4, which is basically responsible for increasing the oxygen content on CCC surface and decreasing adversely the surface area and pore volume [24].

3.1.2. XRD analysis of CCC

The XRD pattern of the CCC is shown in Fig. 1. XRD pattern is indexed based on a standard diffraction reference pattern (JCPDS no. 89-8487). Appearance of a broad diffraction background and the absence of a sharp peak reveal a predominantly amorphous structure [38]. Overall, there were two XRD peaks at 2θ = 24° (002) and 2θ = 42° (101) in the spectrum. These signatures relate to crystalline carbon with expanded lattice parameters (carbon with impurities). Apart from the amorphous and crystalline carbon phases, diffraction peaks originating from unidentified impurity phases were also observed in the diffraction patterns at 2θ = 26° (probably traces of quartz) and 2θ = 35°.

Table 1
Physicochemical characteristics of the carbonized corn cob (CCC)

Typical properties	Values
Total pore volume (cm^3/g)	0.005
Mean pore diameter (nm)	11.534
BET surface area (m^2/g)	1.653
Ultimate analysis (wt. %)	
C	49.87
H	3.68
N	0.90
S	Not detected

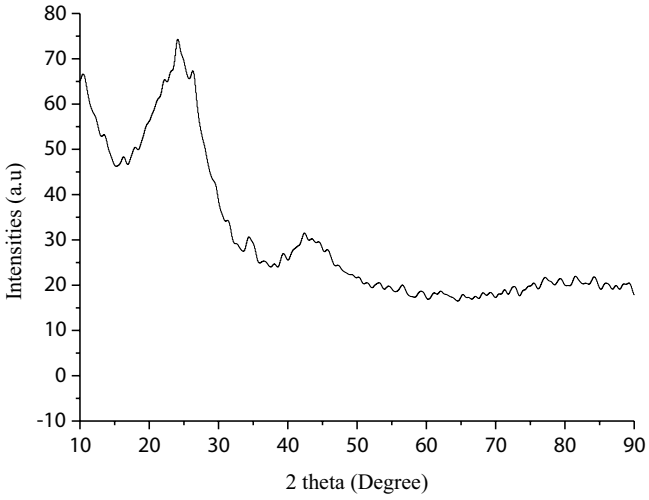

Fig. 1. XRD pattern of carbonized corn cob (CCC).

3.1.3. FTIR spectral analysis

The pattern of MB adsorption onto CCC is related to the availability of active functional groups and bonds of the CCC surface. For the elucidation of these active sites, FTIR spectral analysis was performed. Several infrared (IR) bands appearing in the FTIR spectrum of CCC before adsorption (Fig. 2(a)) were assigned to various functional groups, in accordance with their respective wavenumber (cm^{-1}) position as reported in literature. The weak band observed around 3,500 cm^{-1} is assigned to the overlapping of the stretching vibration of N–H and O–H functional groups [39]. The band at about 1,700 cm^{-1} relates to C=O stretching of ketones, aldehydes, lactones, or carboxyl groups, and the band at 1,600–1,580 cm^{-1}

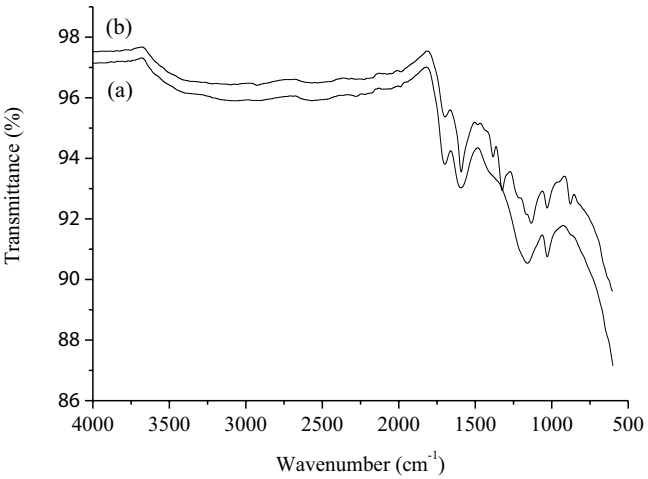

Fig. 2. FTIR spectra of carbonized corn cob (CCC): (a) before and after (b) methylene blue (MB) adsorption.

is assigned to C=C vibrations in aromatic rings [7]. The IR bands between 1,300 and 1,000 cm^{-1} are observed for oxidized carbon materials and are assigned to C–O and/or C–O–C stretching in acids, alcohols, phenols, ethers, and/or esters groups [17,39,40]. Thus, the FTIR spectrum of CCC before adsorption indicates that the external surface of CCC is rich-SO_3H group in addition to various functional groups, containing oxygen of carboxylic and carbonyl species. These active groups on CCC surface are responsible for enhancing the adsorption of cationic species such as MB due to the electrostatic interaction. After MB adsorption, new IR bands appear and many functional groups have undergone red or blue shifting (Fig. 2(b)). New bands assigned to anhydride at ~1,400 cm^{-1} and nitro at ~1,300 cm^{-1} are attributed to MB molecules loaded onto CCC surface.

3.1.4. Surface morphology of CCC

The changes in the surface morphology of CCC before and after MB adsorption are shown in Figs. 3(a) and 3(b), respectively. The SEM image reveals that the surface of CCC before adsorption (Fig. 3(a)) is highly heterogeneous. Pores with different size and shape are also clearly visible. The resulting pore structure is suitable for the adsorption of MB within the pore structure of CCC. This assumption is confirmed by Fig. 3(b) where the CCC surface is altered to be denser and less open pores are seen on the surface of CCC after MB adsorption.

3.1.5. Point-of-zero charge

The pH_{pzc} of the CCC (Fig. 4) was 4.0, which indicates the acid character of the CCC surface, in agreement with the presence of acid groups from the FTIR results (Fig. 2(a)). Generally, adsorption of anions is favored at solution pH below the pH_{pzc} value as the surface of CCC is positively charged due to protonation, whereas at solution pH above the pH_{pzc} value, the surface of CCC becomes negatively charged and thus, adsorption of cations is preferred. In this respect, Jawad et al. reported that the pH_{pzc} values of the coconut leaf and mango peel treated with H_2SO_4

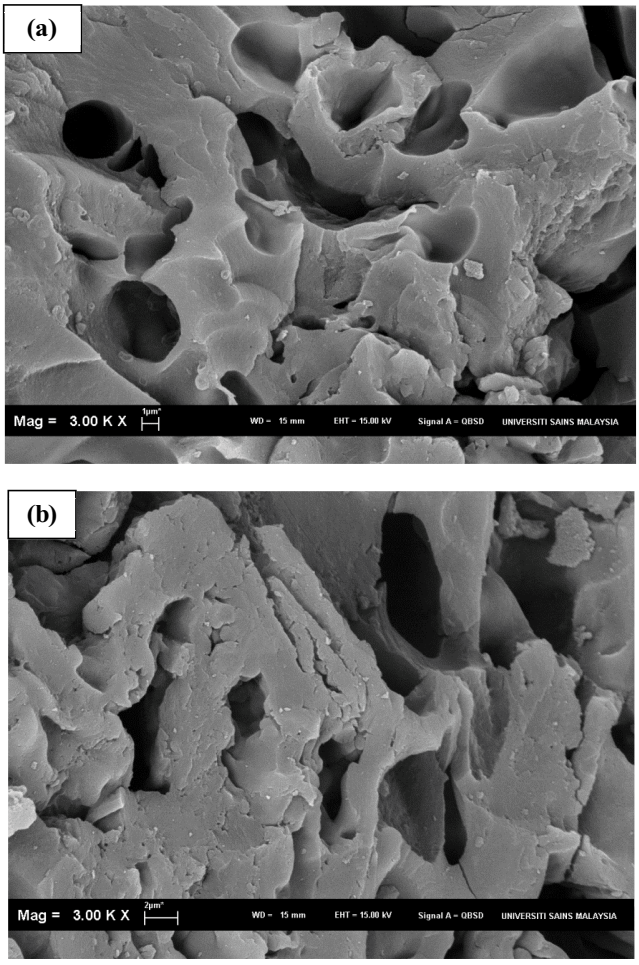

Fig. 3. Typical scanning electron micrograph (SEM) of carbonized corn cob (CCC) particle: (a) before and after (b) methylene blue (MB) adsorption.

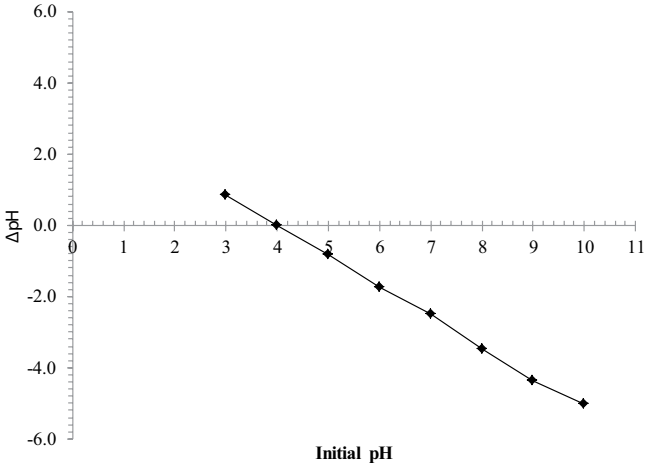

Fig. 4. pH_{pzc} of carbonized corn cob (CCC) suspensions.

were 3.20 [17] and 4.60 [21], respectively. Furthermore, Karagöz et al. [30] reported that the pH_{pzc} value of AC derived from sunflower oil cake treated with H_2SO_4 lies between pH 2.5 and 5.5.

3.2. MB adsorption

3.2.1. Effect of the adsorbent dosage

The effect of adsorbent dosage on the removal of the MB from aqueous solution was determined using variable quantities of CCC adsorbent ranging from 0.02 to 0.20 g at fixed volumes (100 mL) and initial dye solution where C_o was 100 mg/L. For these experiments, other operation parameters were held constant at 303 K, shaking speed of 110 stroke/min, contact time of 60 min, and an unadjusted pH at 5.60 for the initial MB solution. The results are shown in Fig. 5. The highest level of MB removal was achieved using 0.12 g CCC and further addition has not significantly affected the MB removal percentage. The observed increase in the dye removal (%) with adsorbent dosage was attributed to an increase in the available adsorbent surface area, as the number of adsorption sites increase correspondingly. However, no significant changes in MB removal efficiency were observed beyond 0.12 g/100 mL CCC dose. Therefore, 0.12 g of CCC was selected for subsequent work.

3.2.2. Effect of pH

The pH of the solution influences the speciation of the dyes, along with the surface charge of the adsorbent. Fig. 6 shows the effect of variable pH from 3 to 10 on the adsorption capacity with MB. The removal of MB increased slowly as the pH of the solution increased from 3 up to 5, where no remarkable change was observed by increasing the pH to an alkaline environment. MB uptake (q_e) onto CCC was not affected by pH within the range from 3 to 10 due to buffering effect of the adsorbent [41]. Similar observations have been reported for the adsorption of MB by H_2SO_4 treated coconut leaves [17] and mango peel [21]. Therefore, the pH value of unadjusted MB solution (pH 5.6) was used throughout this study.

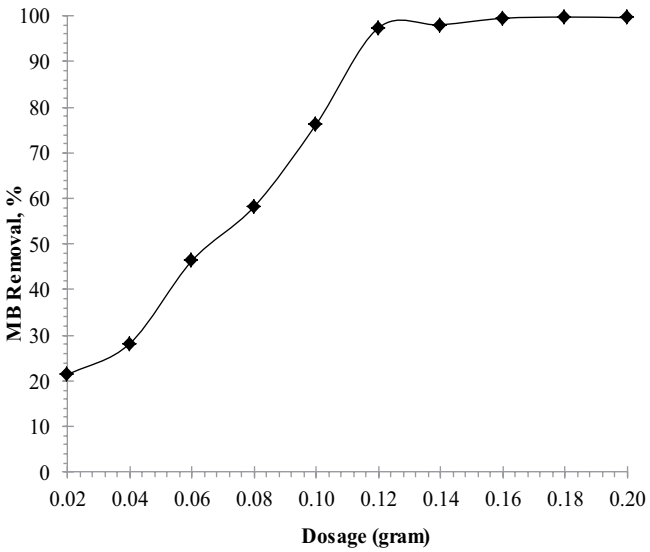

Fig. 5. Effect of carbonized corn cob (CCC) dosage on MB removal (%) at $[MB]_o$ = 100 mg/L, V = 100 mL, pH = 5.6, T = 303 K, shaking speed = 110 stroke/min, and contact time = 60 min.

3.2.3. Effect of initial dye concentration and contact time

The experimental results for the adsorption properties of MB onto CCC at various initial concentrations are shown in Fig. 7. The amount of MB adsorbed by the CCC adsorbent at equilibrium increased rapidly from 39.1 to 250.7 mg/g as the initial dye concentration increased from 50 to 300 mg/L. Indeed, the resistance to mass transfer between the solid and aqueous phase is more easily overcome due to the

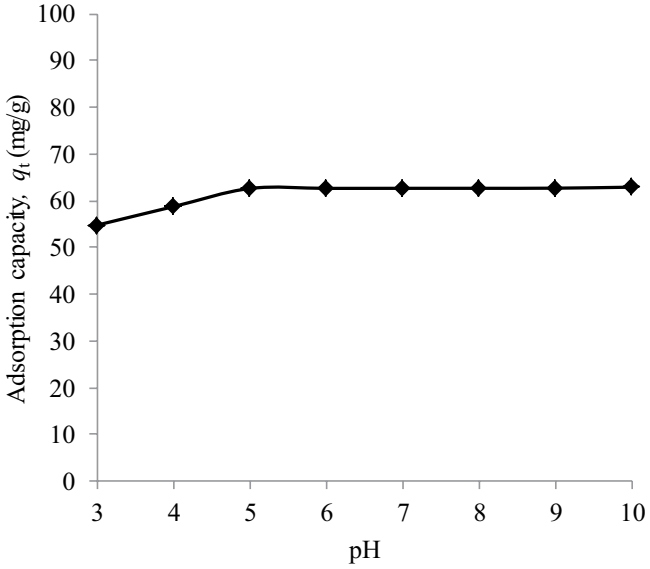

Fig. 6. Effect of pH on the adsorption capacity of MB by CCC at $[MB]_o$ = 100 mg/L, V = 100 mL, T = 303 K, shaking speed = 110 stroke/min, contact time = 24 h, and CCC dosage = 0.12 g.

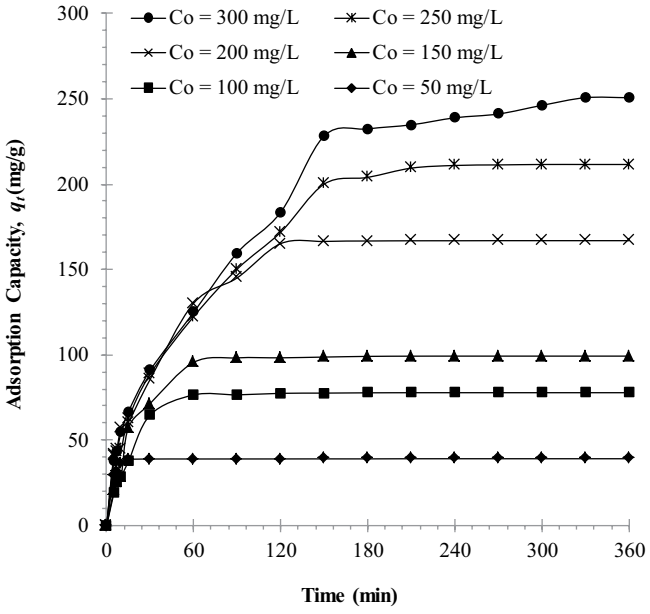

Fig. 7. Effect of initial concentration and contact time on the adsorption of MB by carbonized corn cob (CCC) at V = 100 mL, T = 303 K, pH = 5.6, shaking speed = 110 stroke/min, and CCC dosage = 0.12 g.

driving forces. The effect can be attributed to the greater rate of collision rate between MB and CCC surface at higher initial dye concentration. Hence, additional amounts of MB were transferred to the CCC surface. Additional time was needed to reach equilibrium for higher dye concentration because there was a tendency for MB to penetrate deeper within the interior surface of the CCC and be adsorbed at active pore sites. This indicates that the initial dye concentration plays a significant role in the adsorption capacity of MB onto CCC sorbent.

3.2.4. Effect of temperature on MB adsorption

Temperature is anticipated to have an influence on the dye adsorption properties of CCC adsorbent with MB. The effect of temperature on the dye adsorption properties at 313, 323, and 333 K with fixed initial MB concentration of 50 mg/L was investigated, as shown in Fig. 8. The adsorption capacity of the CCC increased when the temperature increased from 313 to 333 K. The uptake of MB onto CCC was rapid initially and then slowed down gradually until it attained equilibrium beyond which there was no significant increase in the MB uptake. The observed result indicates that the adsorption process of MB onto CCC was favored at higher temperature, in agreement with an endothermic adsorption process. This can be partly attributed to strong attractive forces between MB and CCC at higher temperatures [42], along with the contributions due to desolvation of the CCC surface. It can also be said that reaction of dye molecules and surface functional groups is enhanced by increased temperature of reaction [43].

3.3. Adsorption isotherm

Adsorption isotherm is used to describe adsorbent–adsorbate interaction and the equilibrium distribution of adsorbate molecules at the solid–liquid phases [37]. The adsorption equilibrium was determined by plotting the experimental amount of MB adsorbed q_e (mg/g), against the dye concentration, C_e (mg/L), under equilibrium conditions as shown in Fig. 9. The adsorption equilibrium was further evaluated using three isotherm models, namely Langmuir, Freundlich, and Temkin. The Langmuir isotherm model [44] describes the monolayer adsorption process on uniform adsorption sites and can be expressed by the following equation:

$$q_e = \frac{q_{\max} K_a C_e}{1 + K_a C_e} \tag{4}$$

where q_e is the equilibrium adsorbed amount in mg/g, C_e is the equilibrium concentration in mg/L, $q_{\max}$ is the Langmuir maximum adsorption capacity, and K_a is the Langmuir constant that is linked to adsorption energy. The essential features of Langmuir adsorption isotherm parameter can be used to predict the affinity between the sorbate and sorbent using a dimensionless constant called separation factor or equilibrium parameter (R_L) [45], which is expressed by the following equation:

$$R_L = \frac{1}{1 + K_L C_o} \tag{5}$$

An adsorption system is considered favorable when $0 < R_L < 1$, unfavorable when $R_L > 1$, linear when $R_L = 1$, or irreversible when $R_L = 0$. In this work, the values of R_L obtained were between 0 and 1 and indicate that the adsorption process is favorable for the CCC–MB system. The calculated R_L values at different initial MB concentrations are shown in Table 2. Alternatively, the Freundlich equation is an empirical equation proposed by Freundlich [46] to describe the sorption behavior of solute concentration on heterogeneous surface, expressed by the following equation:

$$q_e = K_f C_e^{1/n} \tag{6}$$

where K_f is the Freundlich coefficient that explains the adsorption capacity and $1/n$ is the Freundlich exponential coefficient that describes the intensity of the adsorption.

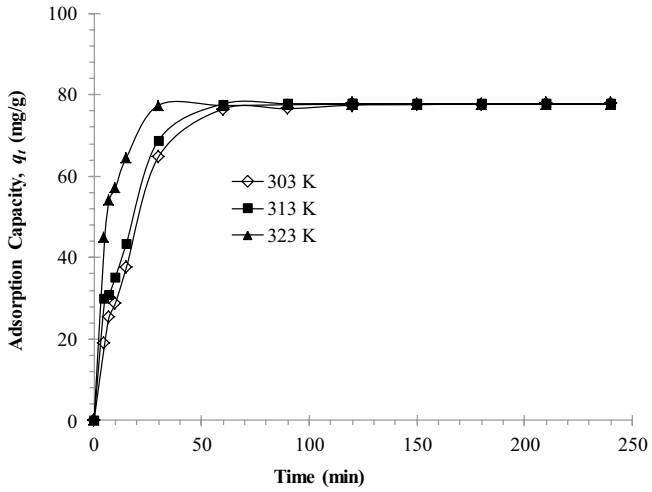

Fig. 8. Effect of temperature on the adsorption of MB by carbonized corn cob (CCC) at $[MB]_o$ = 100 mg/L, V = 200 mL, pH = 5.6, shaking speed = 110 stroke/min, and CCC dosage = 0.12 g.

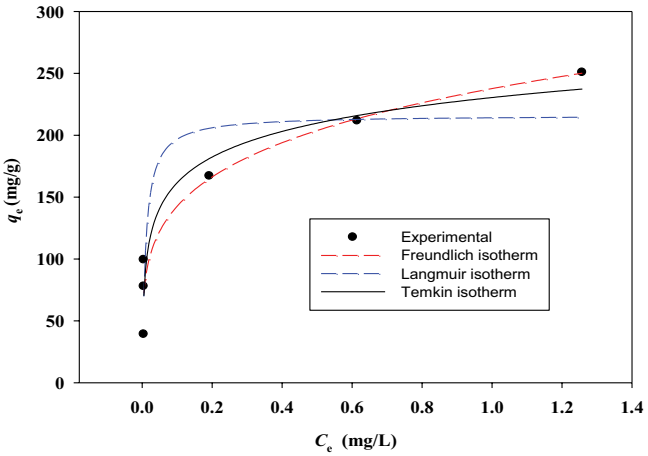

Fig. 9. Sorption data of methylene blue (MB) on carbonized corn cob (CCC), with best-fit Langmuir, Freundlich, and Temkin models.

Table 2
Dimensionless constant separation factor, R_L for adsorption of methylene blue (MB) onto carbonized corn cob (CCC) at various initial MB concentrations

Parameter	Concentrations, C_o (mg/L)					
$R_L \times 10^{-4}$	50	100	150	200	250	300
	9.99	5.00	3.33	2.50	2.00	1.67

Temkin isotherm [47] deals with adsorbent–adsorbate interactions and their effect on linear decrease of heat of adsorption with coverage, expressed in the following equation:

$$q_e = B\ln\left(AC_e\right) \tag{7}$$

where $B = RT/b$ and corresponds to enthalpy of adsorption, b is Temkin constant related to heat of sorption (J/mol), and A is binding constant at equilibrium which corresponds to the maximum binding energy (L/g).

The nonlinear plots of the Langmuir, Freundlich, and Temkin models are presented in Fig. 9, and their corresponding isotherm values are shown in Table 3. Based on calculated data, Freundlich model fits the data better than Temkin and Langmuir models. This result is confirmed by the high R^2 value for the Freundlich model (0.9448) compared with the Temkin (0.9328) and Langmuir (0.8613) models. Freundlich isotherm indicates multilayer heterogeneous adsorbent surface with different adsorption sites [48].

Table 3
Parameters of the Langmuir, Freundlich, and Temkin nonlinear isotherm models for MB adsorption on CCC surface at 303 K, fit in their original, nonlinear forms

Isotherm	Parameter	Value
Langmuir	q_m (mg/g)	216.2
	K_a (L/mg)	101.3
	R^2	0.8613
Freundlich	K_F ((mg/g) (L/mg)$^{1/n}$)	237.7
	n	4.5
	R^2	0.9448
Temkin	K_T (L/mg)	2.2×10^3
	B_T	29.9
	R^2	0.9328

A value of $1/n > 1$ suggests weak adsorption bond between MB molecules onto CCC particles; on the other hand, a value of $1/n < 1$ suggests strong adsorption bond as a result of strong intermolecular attraction within the adsorbent layers [49]. The value of n range from 2 and 10 indicates good adsorption when the value of 4–5 indicates good adsorption capacity and less than 1 indicating undesirable adsorption capacity [50]. The maximum monolayer adsorption capacity of MB onto surface of CCC at equilibrium was determined by Langmuir model to be 216.2 mg/g at 303 K. The monolayer adsorption capacity (q_{max}) for CCC with MB was compared with other types of H_2SO_4-treated lignocellulosic materials as recorded in Table 4. The foregoing indicates that CCC represents a promising renewable and low-cost biochar for removing cationic dyes such as MB.

3.4. Adsorption kinetics

The rate and mechanism of the adsorption process was evaluated using the nonlinear pseudo-first-order (PFO) model and pseudo-second-order (PSO) model. The PFO model was proposed initially by Lagergren [51] and is expressed by Eq. (8) as follows:

$$q_t = q_e\left(1 - \exp^{-K_1 t}\right) \tag{8}$$

q_e (mg/g) and q_t (mg/g) are the amounts of MB adsorbed by CCC at equilibrium and time t, respectively, while k_1 (min^{-1}) is the PFO rate constant. The nonlinear form of the PSO model [52] is described by Eq. (9) as follows:

$$q_t = \frac{q_e^2 k_2 t}{1 + q_e k_2 t} \tag{9}$$

The kinetic data were fit to the nonlinear form of kinetic models; hence, the best fitted model was also evaluated

Table 4
Adsorption capacities for methylene blue (MB) onto different biomass materials treated with H_2SO_4 acid

Biomass treated with H_2SO_4	Adsorbent dosage (g)	pH	Temperature (K)	q_{max} (mg/g)	References
Corn cob	0.12 g/100 mL	5.6	303	216.2	This study
Pine-fruit shell	0.3 g/100 mL	8.5	298	529	[31]
Mango peels	0.14 g/100 mL	5–6	303	277.80	[21]
Coconut leaves	0.15 g/100 mL	6	303–323	126.90–149.30	[17]
Euphorbia rigida	0.2 g/100 mL	6	293–313	114	[26]
Bagasse	0.4 g/100 mL	9	300–333	49.8–56.5	[27]
Ficus carica	0.5 g/100 mL	8	298–323	47.62	[34]
Parthenium hysterophorus	0.4 g/100 mL	7	298	39.7	[29]
Delonix regia pods	0.2 g/100 mL	7	298	23.30	[32]
Wild carrot	0.05 g/100 mL	6	298	21.00	[33]
Sunflower oil cake	0.2 g/100 mL	6	288–318	16.43	[30]

by nonlinear coefficient of determination (R^2). The plots of two nonlinear kinetic models are depicted in Fig. 10. Additionally, the kinetic parameters of these two models at different concentrations with their corresponding R^2 are given in Table 5. From Table 5, the PFO model has a relatively high R^2 values compared with the R^2 values obtained from PSO model. This suggests that the amount of adsorbed MB increases with increasing adsorption time and approaching a constant adsorbed amount after saturation [50]. Moreover, the $q_{t\text{-meas}}$ values fitted well with the $q_{t\text{-exp}}$ values. Thus, the PFO model is more suitable to describe a physical adsorption process of MB onto CCC surface.

3.5. Adsorption thermodynamics

The thermodynamic adsorption parameters of MB onto CCC were computed from the experimental data obtained at 313, 323, and 333 K. Gibb's free energy ($\Delta G°$), enthalpy ($\Delta H°$), and entropy ($\Delta S°$) were calculated using the following equations [53]:

$$k_d = \frac{q_e}{C_e} \tag{10}$$

$$\Delta G° = \Delta H° - T\Delta S° \tag{11}$$

$$\ln k_d = \frac{\Delta S°}{R} - \frac{\Delta H°}{RT} \tag{12}$$

where k_d is the distribution coefficient, q_e is the concentration of MB adsorbed on CCC at equilibrium (mg/L), C_e is the equilibrium concentration of MB in the liquid phase (mg/L), R is the universal gas constant (8.314 J/mol K), and T is the absolute temperature (K). The values of $\Delta H°$ and $\Delta S°$ were calculated from the slope and intercept of van't Hoff plots of ln k_d versus $1/T$ respectively (Fig. 11). The thermodynamic parameters are listed in Table 6. In general, the value for $\Delta G°$, energy for physisorption ranges from −20 to 0 kJ/mol, the physisorption together with chemisorption falls at the range of −20 to −80 kJ/mol and chemisorption is more negative in magnitude with a range of −80 to −400 kJ/mol [54]. The negative values of $\Delta G°$ indicate spontaneous and favorable MB adsorption onto the surface of CCC [55]. The positive value of the enthalpy change ($\Delta H°$ = 25.5 kJ/mol) indicates that the adsorption process is endothermic in nature. The positive

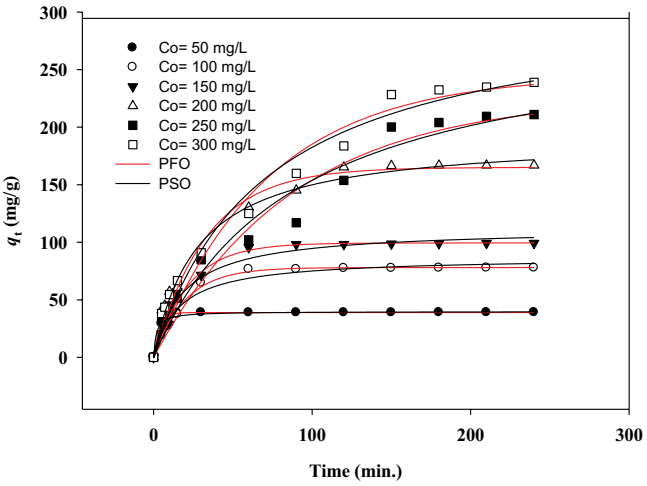

Fig. 10. Nonlinear kinetic profiles of PFO and PSO for the adsorption of MB onto carbonized corn cob (CCC).

Table 5
Parameters of the nonlinear PFO and PSO kinetic models for MB adsorption on carbonized corn cob (CCC) at different initial methylene blue (MB) concentrations

Parameters	C_o (mg/L)					
	50	100	150	200	250	300
$q_{e,\text{exp}}$ (mg/g)	39.1	77.8	99.3	166.9	211.5	250.7
PFO						
$q_{e,\text{meas}}$ (mg/g)	39.0	78.1	99.4	165.09	226.05	245.4
k_1 (min^{-1})	0.2631	0.0510	0.0455	0.0302	0.0114	0.0141
R^2	0.9984	0.9951	0.9917	0.9763	0.9496	0.9692
PSO						
$q_{e,\text{meas}}$ (mg/g)	39.8	87.1	112.2	191.6	290.6	311.5
$k_2 \times 10^{-4}$ (g/mg min)	14.7	7.2	4.8	1.8	38.5	45.5
R^2	0.9370	0.9787	0.9778	0.9864	0.9581	0.9779

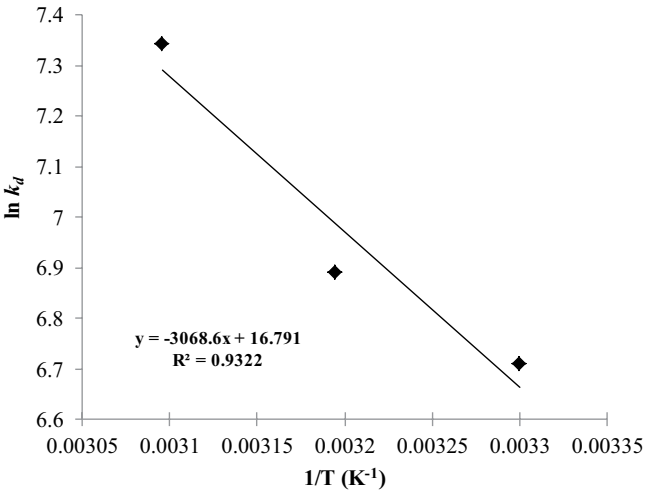

Fig. 11. Plot of ln k_d versus $1/T$ for calculation of thermodynamic parameters for the adsorption of MB onto CCC.

Table 6
Thermodynamic parameters values for the adsorption of methylene blue (MB) onto carbonized corn cob (CCC)

Temperature (K)	Thermodynamics			
	k_d	$\Delta G°$ (kJ/mol)	$\Delta H°$ (kJ/mol)	$\Delta S°$ (J/mol K)
313	821.5	−67.80		
323	982.2	−69.20	25.5	139.6
333	1,542.8	−70.50		

entropy change ($\Delta S°$) value of 139.6 J/mol K corresponds to increase in the degree of freedom of the adsorbed species due to adsorbate disorder and/or loss of water upon binding of MB to the CCC surface.

4. Conclusion

This research work clearly shows that carbonization of corn cob (CC) by H_2SO_4 activation provides a low-cost adsorbent for the removal of MB dye from aqueous solutions. The adsorption experiments indicated that the PFO model provided the best description of the kinetic uptake properties, while adsorption results at equilibrium are described by the Freundlich model. The maximum adsorption capacity (q_{max}) calculated from nonlinear Langmuir isotherm was 216.2 mg/g. The thermodynamic parameters indicate that the adsorption process is endothermic in nature and driven by entropy to yield a spontaneous adsorption process. The results indicated that carbonized corn cob (CCC) is an efficient adsorbent for MB adsorption.

Acknowledgment

The authors would like to thank institute of research management and innovation (IRMI) for supporting this project under Geran Insentif Penyeliaan (GIP) grant (600-IRMI/MyRA 5/3/GIP (055/2017)).

References

[1] N.S.A. Mubarak, A.H. Jawad, W.I. Nawawi, Equilibrium, kinetic and thermodynamic studies of Reactive Red 120 dye adsorption by chitosan beads from aqueous solution, Energy Ecol. Environ., 2 (2017) 85–93.
[2] A.H. Jawad, M.A.M. Ishak, A.M. Farhan, K. Ismail, Response surface methodology approach for optimization of color removal and COD reduction of methylene blue using microwave-induced NaOH activated carbon from biomass waste, Desal. Wat. Treat., 62 (2017) 208–220.
[3] A.H. Jawad, N.S.A. Mubarak, W.I. Nawawi, Optimization of Sorption Parameters for Color Removal of Textile Dye by Cross-Linked Chitosan Beads Using Box-Behnken Design, MATEC Web of Conferences, 47, 05009, 2016.
[4] R. Juang, S. Swei, Effect of dye nature on its adsorption from aqueous solution onto activated carbon, Sep. Sci. Technol., 31 (1996) 2143–2158.
[5] A.H. Jawad, R.A. Rashid, R.M.A. Mahmuod, M.A.M. Ishak, N.N. Kasim, K. Ismail, Adsorption of methylene blue onto coconut (*Cocos nucifera*) leaf: optimization, isotherm and kinetic studies, Desal. Wat. Treat., 57 (2016) 8839–8853.
[6] A.H. Jawad, S. Sabar, M.A.M. Ishak, L.D. Wilson, S.S.A. Norrahma, M.K. Talari, A.M. Farhan, Microwave-assisted preparation of mesoporous activated carbon from coconut (*Cocos nucifera*) leaf by H_3PO_4-activation for methylene blue adsorption, Chem. Eng. Commun., 204 (2017) 1143–1156.
[7] A.H. Jawad, R.A. Rashid, K. Ismail, S. Sabar, High surface area mesoporous activated carbon developed from coconut leaf by chemical activation with H_3PO_4 for adsorption of methylene blue, Desal. Wat. Treat., 74 (2017) 326–335.
[8] A.R. Khataee, A. Movafeghi, S. Torbati, S.Y. SalehiLisar, M. Zarei, Phytoremediation potential of duckweed (*Lemna minor* L.) in degradation of C.I. Acid Blue 92: artificial neural network modeling, Ecotoxicol. Environ. Saf., 80 (2012) 291–298.
[9] L. Fan, Y. Zhou, W. Yang, G. Chen, F. Yang, Electrochemical degradation of aqueous solution of Amaranth azo dye on ACF under potentiostatic model, Dyes Pigm., 76 (2008) 440–446.
[10] J.S. Wu, C.H. Liu, K.H. Chu, S.Y. Suen, Removal of cationic dye methyl violet 2B from water by cation exchange membranes, J. Membr. Sci., 309 (2008) 239–245.
[11] Y.S. Woo, M. Rafatullah, A.F.M. Al-Karkhi, T.T. Tow, Removal of Terasil Red R dye by using Fenton oxidation: a statistical analysis, Desal. Wat. Treat., 52 (2014) 4583–4591.
[12] A.H. Jawad, A.F.M. Alkarkhi, N.S.A. Mubarak, Photocatalytic decolorization of methylene blue by an immobilized TiO_2 film under visible light irradiation: optimization using response surface methodology (RSM), Desal. Wat. Treat., 56 (2015) 161–172.
[13] A.H. Jawad, N.S.A. Mubarak, M.A.M. Ishak, K. Ismail, W.I. Nawawi, Kinetics of photocatalytic decolourization of cationic dye using porous TiO_2 film, J. Taibah Univ. Sci., 10 (2016) 352–362.
[14] F. Akbal, Adsorption of basic dyes from aqueous solution onto pumice powder, J. Colloid Interface Sci., 286 (2005) 455–458.
[15] A.H. Jawad, M.A. Islam, B.H. Hameed, Cross-linked chitosan thin film coated onto glass plate as an effective adsorbent for adsorption of reactive orange 16, Int. J. Biol. Macromol., 95 (2017) 743–749.
[16] J. Xu, L. Chen, H. Qu, Y. Jiao, J. Xie, G. Xing, Preparation and characterization of activated carbon from reedy grass leaves by chemical activation with H_3PO_4, Appl. Surf. Sci., 320 (2014) 674–680.
[17] A.H. Jawad, R.A. Rashid, M.A.M. Ishak, L.D. Wilson, Adsorption of methylene blue onto activated carbon developed from biomass waste by H_2SO_4 activation: kinetic, equilibrium and thermodynamic studies, Desal. Wat. Treat., 57 (2016) 25194–25206.
[18] F. Marrakchi, M.J. Ahmed, W.A. Khanday, M. Asif, B.H. Hameed, Mesoporous-activated carbon prepared from chitosan flakes via single-step sodium hydroxide activation for the adsorption of methylene blue, Int. J. Biol. Macromol., 98 (2017) 233–239.
[19] L. Gao, F. Dong, Q. Dai, G. Zhong, U. Halik, D. Lee, Coal tar residues based activated carbon: preparation and characterization, J. Taiwan Inst. Chem. Eng., 63 (2016) 166–169.
[20] R. Acosta, V. Fierro, A.M. Yuso, D. Nabarlatz, A. Celzard, Tetracycline adsorption onto activated carbons produced by KOH activation of tyre pyrolysis char, Chemosphere, 149 (2016) 168–176.
[21] A.H. Jawad, N.F.H. Mamat, M.F. Abdullah, K. Ismail, Adsorption of methylene blue onto acid-treated Mango peels: kinetic, equilibrium and thermodynamic, Desal. Wat. Treat., 59 (2017) 210–219.
[22] Q.S. Liu, T. Zheng, N. Li, P. Wang, G. Abulikemu, Modification of bamboo-based activated carbon using microwave radiation and its effects on the adsorption of methylene blue, Appl. Surf. Sci., 256 (2016) 3309–3315.
[23] Y. Gokce, Z. Aktas, Nitric acid modification of activated carbon produced from waste tea and adsorption of methylene blue and phenol, Appl. Surf. Sci., 313 (2014) 352–359.
[24] H. Valdes, M. Sanchez-Polo, J. Rivera-Utrilla, C.A. Zaror, Effect of ozone treatment on surface properties of activated carbon, Langmuir, 18 (2002) 2111–2116
[25] Q. Cao, K.C. Xie, Y.K. Lv, W.R. Bao, Process effects on activated carbon with large specific surface area from corn cob, Bioresour. Technol., 97 (2006) 110–115.
[26] Ö. Gerçel, A. Özcan, A.S. Özcan, H.F. Gerçel, Preparation of activated carbon from a renewable bio-plant of *Euphorbia rigida* by H_2SO_4 activation and its adsorption behavior in aqueous solutions, Appl. Surf. Sci., 253 (2007) 4843–4852.
[27] L.W. Low, T.T. Teng, A. Ahmad, N. Morad, Y.S. Wong, A novel pretreatment method of lignocellulosic material as adsorbent and kinetic study of dye waste adsorption, Water, Air, Soil, Pollut., 218 (2011) 293–306.
[28] H. Hasar, Adsorption of nickel (II) from aqueous solution onto activated carbon prepared from almond husk, J. Hazard. Mater., 97 (2003) 49–57.
[29] H. Lata, V.K. Garg, R.K. Gupta, Removal of a basic dye from aqueous solution by adsorption using *Parthenium hysterophorus*: an agricultural waste, Dyes Pigm., 74 (2007) 653–658.
[30] S. Karagöz, T. Tay, S. Ucar, M. Erdem, Activated carbons from waste biomass by sulfuric acid activation and their use on methylene blue adsorption, Bioresour. Technol., 99 (2008) 6214–6222.

[31] B. Royer, N.F. Cardoso, E.C. Lima, J.C.P. Vaghetti, R.C. Veses, Applications of Brazilian pine-fruit shell in natural and carbonized forms as adsorbents to removal of methylene blue from aqueous solutions: kinetics and equilibrium study, J. Hazard. Mater., 164 (2009) 1213–1222.
[32] Y.S. Ho, R. Malaryvizhi, N. Sulochana, Equilibrium isotherm studies of methylene blue adsorption onto activated carbon prepared from *Delonix regia* pods, J. Environ. Prot. Sci., 3 (2009) 1–6.
[33] M. Mahadeva Swamy, B.M. Nagabhushana, R. Hari Krishna, Nagaraju Kottam, R.S. Raveendra, P.A. Prashanth, Fast adsorptive removal of methylene blue dye from aqueous solution onto a wild carrot flower activated carbon: isotherms and kinetics studies, Desal. Wat. Treat., 71 (2017) 399–405.
[34] D. Pathania, S. Sharma, P. Singh, Removal of methylene blue by adsorption onto activated carbon developed from *Ficus carica* bast, Arabian J. Chem., 10 (2017) S1445–S1451.
[35] N. Sharma, D.P. Tiwari, S.K. Singh, The efficiency appraisal for removal of malachite green by potato peel and neem bark: isotherm and kinetic studies, Int. J. Chem. Environ. Eng., 5 (2014) 83–88.
[36] V.K. Garg, R. Kumar, R. Gupta, Removal of malachite green dye from aqueous solution by adsorption using agro-industry waste: a case study of *Prosopis cineraria*, Dyes Pigm., 62 (2004) 1–10.
[37] M.V. Lopez-Ramon, F. Stoeckli, C. Moreno-Castilla, F. Carrasco-Marin, On the characterization of acidic and basic surface sites on carbons by various techniques, Carbon, 37 (1999) 1215–1221.
[38] P. Barpanda, G. Fanchini, G.G. Amatucci, Structure, surface morphology and electrochemical properties of brominated activated carbons, Carbon, 49 (2011) 2538–2548.
[39] A.H. Jawad, M.A. Nawi, Characterizations of the photocatalytically-oxidized cross-linked chitosan-glutaraldehyde and its application as a sub-layer in the TiO_2/CS-GLA bilayer photocatalyst system, J. Polym. Environ., 20 (2012) 817–829.
[40] R.A. Rashid, A.H. Jawad, M.A.M. Ishak, N.N. Kasim, KOH-activated carbon developed from biomass waste: adsorption equilibrium, kinetic and thermodynamic studies for Methylene blue uptake, Desal. Wat. Treat., 57 (2016) 27226–27236.
[41] K.C. Bedin, A.C. Martins, A.L. Cazetta, O. Pezoti, V.C. Almeida, KOH-activated carbon prepared from sucrose spherical carbon: adsorption equilibrium, kinetic and thermodynamic studies for Methylene Blue removal, Chem. Eng. J., 286 (2015) 476–484.
[42] W.T. Tsai, C.W. Lai, K.J. Hsien, Adsorption kinetics of herbicide paraquat from aqueous solution onto activated bleaching earth, Chemosphere, 55 (2004) 829–837.
[43] A.E. Ofomaja, Sorption dynamics and isotherm studies of methylene blue uptake on to palm kernel fibre, Chem. Eng. J., 126 (2007) 35–43.
[44] I. Langmuir, The adsorption of gases on plane surfaces of glass, mica and platinum, J. Am. Chem. Soc., 40 (1918) 1361–1403.
[45] K.R. Hall, L.C. Eagleton, A. Acrivos, T. Vermeulen, Pore- and solid diffusion kinetics in fixed-bed biosorption under constant-pattern conditions, Ind. Eng. Chem. Fundam., 5 (1966) 212–223.
[46] H. Freundlich, Ueber die adsorption in Loesungen (Adsorption in solution), Z. Phys. Chem., 57 (1906) 385–470.
[47] M.J. Temkin, V. Pyzhev, Recent modifications to Langmuir isotherms, Acta Physiochim. USSR, 12 (1940) 217–222.
[48] I. Vázquez, J. Rodríguez-Iglesias, E. Marañón, L. Castrillón, M. Álvarez, Removal of residual phenols from coke wastewater by adsorption, J. Hazard. Mater., 147 (2007) 395–400.
[49] D. Duong, Adsorption Analysis Equilibria and Kinetics 2, Imperial College, London, 1998.
[50] P. Nanta, K. Kasemwong, W. Skolpap, Isotherm and kinetic modeling on superparamagnetic nanoparticles adsorption of polysaccharide, J. Environ. Chem. Eng., 6 (2018) 794–802.
[51] S. Lagergren, Zur theorie der sogenannten adsorption geloster stoffe, K. Sven. Vetenskapsakad. Handl., 24 (1898) 1–39.
[52] Y.S. Ho, G. McKay, Sorption of dye from aqueous solution by peat, Chem. Eng. J., 70 (1998) 115–124.
[53] G. Karacetin, S. Sivrikaya, M. Imamoglu, Adsorption of methylene blue from aqueous solutions by activated carbon prepared from hazelnut husk using zinc chloride, J. Anal. Appl. Pyrolysis, 110 (2014) 270–276.
[54] K.E. Noll, V. Gounaris, W.S. Hou, Adsorption Technology for Air and Water Pollution Control, Lewis Publishers, Chelsea, MI, 1992, pp. 21–22.
[55] Y. Yu, Y.Y. Zhuang, Z.H. Wang, Adsorption of water-soluble dye onto functionalized resin, J. Colloid Interface Sci., 242 (2001) 288–293.